Preprints of the 18th IFAC World Congress
Milano (Italy) August 28 - September 2, 2011

Robust Tool Point Control for Offshore Knuckle Boom Crane

M. K. Bak M. R. Hansen H. R. Karimi

Department of Enginering, Faculty of Engineering and Science, University of Agder, NO-4898 Grimstad, Norway (e-mails: morten.k.bak@uia.no;michael.r.hansen@uia.no;hamid.r.karimi@uia.no)

Abstract: This paper considers the design of an H_∞ controller for tool point control of a hydraulically actuated knuckle boom crane. The paper describes the modelling of the crane's mechanical and hydraulic systems and a disturbance model. These are linearised and combined in a state-space model used for the controller design. The controller synthesis problem is to design (if possible) an admissible controller that solves the problem of robust regulation against step inputs with an H_∞ constraint based on the internal model principle. Simulation results are given to show the effectiveness of the method.

Keywords: Multi-input/multi-output systems, state feedback, robust control.

1. INTRODUCTION

This paper describes a design approach for development of an H_∞ controller for tool point control for an offshore knuckle boom crane used for pipe handling on a drilling rig. The purpose is to achieve robust regulation against step inputs based on the internal model principle.
Offshore equipment in general is constantly exposed to increasing demands regarding productivity, reliability and safety in order to maximise capacity and uptime and to reduce risks of harming equipment, personal and environment. For the considered type of crane, one consequence of this is generally a demand for efficient tool point control.
Tool point control, i.e. direct control of the tool point by automatic coordinated control of the individual DOF (degrees of freedom) as opposed to direct control of each DOF to achieve control of the tool point, has been subjected to research for several years. In the early nineties a simple vector control strategy for a two-DOF crane, like the knuckle boom type, was developed by Krus and Palmberg (1992). Mattila and Virvalo (2000) presented a more advanced control strategy for a similar crane, which reduces energy consumption by reducing pressures levels in the hydraulic system.
Munzer (2003) developed a control scheme for flexible cranes with redundant DOF. Since then, work on similar cranes has been followed by several others. Ebbesen et al. (2006) presented a control strategy based on optimal cylinder velocities determined by minimisation of energy consumption. Recently Pedersen et al. (2010) developed a control scheme by means of dynamic real-time simulation based on a pseudo inverse approach.
These strategies are either purely feedforward based, which yield fast yet still stable response, but in some cases sacrifices tracking performance. Or they involve feedback of several measured signals and need for certain components, which may result in expensive systems.

⋆ The work presented in this paper is funded by the Norwegian Ministry of Education and Research and Aker Solutions.

The goal of the work presented in this paper is to investigate if an H_∞ controller, based on measured signals, can deliver satisfying performance regarding speed and tracking and at the same time remain robust in the presence of disturbances.
H_∞ based design approaches for tracking problems has been developed by Abedor et al. (1995) and furthermore H_∞ control has successfully been applied to numerous crane control problems. Recent examples are control system design for gantry cranes, presented by Burul et al. (2010), controller design for rotary crane, presented by Iwasa et al. (2010), and control of an overhead crane by Moradi et al. (2009).
The theory of H_∞ control is already well established and therefore the work presented in this paper is focused on modelling of the physical system and applying the controller design approach.
The paper is organised in the following way: first the knuckle boom crane and functionality is described. After this the relevant models are established, then linearised and formulated as a state-space model. Next the controller design is presented and finally performance is evaluated by a presentation of simulation results.
Model parameters and comprehensive expressions are given in the appendix.

2. CONSIDERED SYSTEM

The considered knuckle boom crane is used on a semi-submersible drilling rig, i.e. a floating rig that is partially submersed for increased stability. Because the rig is floating its movements act as disturbances on the equipment on board.
The crane is used to move drill pipes between the pipe deck of the rig and a tubular feeding machine, which handles the further transportation of the drill pipes. As illustrated in Fig. 1, the crane consists of five main parts; a pedestal, a rotating part for slewing of the crane, an inner jib, an outer jib and a gripping yoke.

Copyright by the
International Federation of Automatic Control (IFAC)

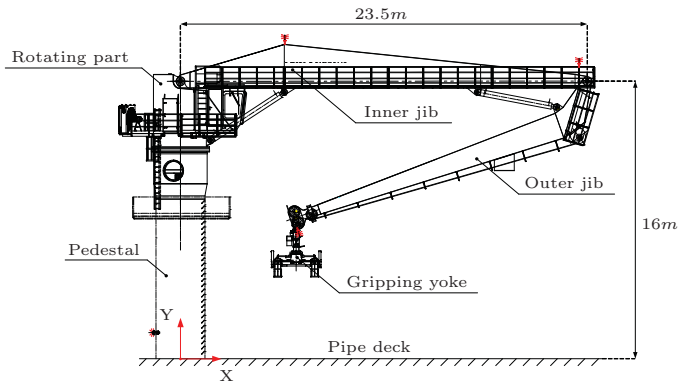

Fig. 1. Offshore knuckle boom crane for pipe handling.

The controller design will focus only on the two-dimensional problem of tool point control, i.e. controlling the planar motion of the tool point. The functionalities of the rotating part and the gripping yoke is not considered.
The inner and outer jibs are actuated by hydraulic cylinders, which must be controlled in a coordinated manner in order to achieve X-Y-motion control of the tool point. The cylinders are controlled as illustrated by Fig. 2, by two pressure compensated proportional directional control valves and counter balance valves for load lowering.

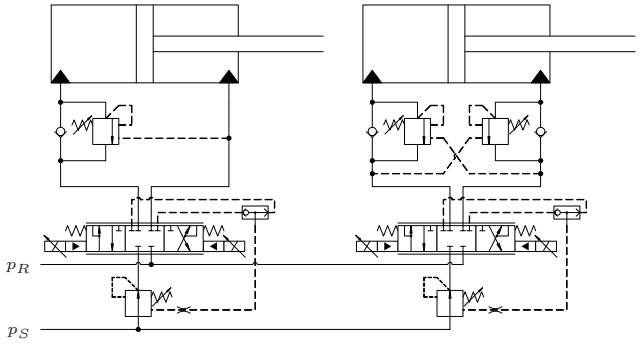

Fig. 2. Hydraulic system for control of the crane jibs.

The system is supplied from a ring-line with constant supply and return pressures p_S and p_R.

3. MODEL DESCRIPTION

The mechanical structure is modelled according to Fig. 3.

The global rotations ϕ_1 and ϕ_2 of the inner and outer jibs and the velocities $\dot{\phi}_1$ and $\dot{\phi}_2$ are chosen as state variables for the mechanical system. For convenience the rotations of the hydraulic cylinder, θ_1 and θ_2, are introduced. These are dependent coordinates, which can be determined when ϕ_1 and ϕ_2 are known.
The dotted red line between the points P_A and P_B represents the operation to be considered - lifting a payload from the pipe deck in a straight vertical motion. When considering this operation, the hydraulic system can be simplified and modelled according to the circuit in Fig. 4.

Cylinder 1 must extend in order to raise the inner jib and cylinder 2 must retract in order to keep point C moving along a straight path. For the given geometric configuration the load force and the velocity of cylinder 2 has the same direction. In practice a certain outlet pressure, p_{r_2}, will be present.

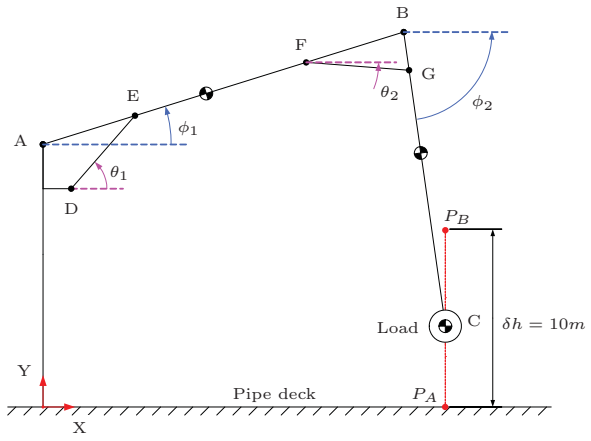

Fig. 3. Simplified geometry of the crane.

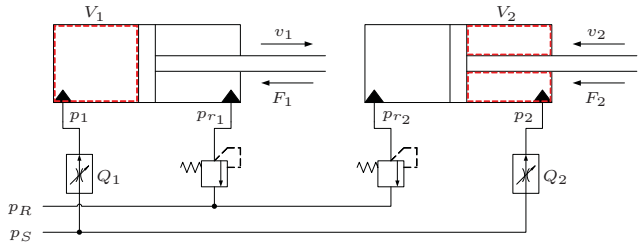

Fig. 4. Simplified hydraulic circuit.

The state variables for the hydraulic system are the pressures p_1 and p_2. The outlet pressures, p_{r_1} and p_{r_2}, can be assumed constant during the operation.
The state variables may be assembled in the state vector:

$$\mathbf{x} = \begin{bmatrix} \phi_1 & \dot{\phi}_1 & \phi_2 & \dot{\phi}_2 & p_1 & p_2 \end{bmatrix}^T \tag{1}$$

3.1 Mechanical System

Since only the state variables and their time derivatives are of interest, the most convenient way to model the mechanical system is by means of Lagrange's equation:

$$\frac{d}{dt}\left\{\frac{\partial L}{\partial \dot{q}_i}\right\} - \frac{\partial L}{\partial q_i} = Q_i^{NC} \tag{2}$$

where $L = T - V$, T being the kinetic energy and V being the potential energy of the system.
In (2) q_i and $\dot{q}_i$ are the generalised coordinates and their time derivatives. In this case ϕ_1 and ϕ_2 are the generalised coordinates.
Q_i^{NC} are the non-conservative generalised forces. In this case they correspond to the moments around points A and B produced by the cylinder forces. They are given by:

$$Q_i^{NC} = \sum_{j=1}^{n} \mathbf{F}_j^{NC} \cdot \frac{\partial \mathbf{r}_j}{\partial q_i} \tag{3}$$

$\mathbf{F}_j^{NC}$ is the force vector at the j'th connection point and $\mathbf{r}_j$ is the position vector to the same point.
Comprehensive expressions for the components of (2)-(3) are given in appendix A.1, A.2 and A.3.
Obtaining the equations of motion yields the following equation system:

$$\begin{bmatrix} a_{11} & a_{12} \\ a_{21} & a_{22} \end{bmatrix} \cdot \begin{bmatrix} \ddot{\phi}_1 \\ \ddot{\phi}_2 \end{bmatrix} = \begin{bmatrix} b_1 \\ b_2 \end{bmatrix} \tag{4}$$

where a_{11} and a_{22} are constant, a_{12} and a_{21} are functions of ϕ_1 and ϕ_2 and b_1 and b_2 are functions of all six state variables. Expressions for these components are given by (A.39)-(A.44) in appendix A.4.
$\ddot{\phi}_1$ and $\ddot{\phi}_2$ can be expressed independently by applying Cramer's rule:

$$\ddot{\phi}_1 = \frac{b_1 \cdot a_{22} - a_{12} \cdot b_2}{D} \tag{5}$$

$$\ddot{\phi}_2 = \frac{a_{11} \cdot b_2 - b_1 \cdot a_{21}}{D} \tag{6}$$

where

$$D = a_{11} \cdot a_{22} - a_{12} \cdot a_{21} \tag{7}$$

3.2 Hydraulic System

By means of the flow continuity equation:

$$Q_{in} - Q_{out} = \dot{V} + \frac{V}{\beta} \cdot \dot{p} \tag{8}$$

the pressure gradients can be expressed as:

$$\dot{p}_1 = \frac{\beta_e \cdot (Q_1 - v_1 \cdot A_{p_1})}{V_1} \tag{9}$$

$$\dot{p}_2 = \frac{\beta_e \cdot (Q_2 + v_2 \cdot CR_2 \cdot A_{p_2})}{V_2} \tag{10}$$

where β_e is the effective stiffness of the hydraulic fluid and A_{p_1} and A_{p_2} are the piston areas for the cylinders.
v_1 and v_2 are the cylinder piston velocities, which are functions of the mechanical state variables. Expressions for the two piston velocities are given by (A.15) and (A.18) in appendix A.1.
Q_1 and Q_2 are the controlled flows given as:

$$Q_1 = u_1 \cdot Q_{max} \tag{11}$$

$$Q_2 = u_2 \cdot Q_{max} \tag{12}$$

where u_1 and u_2 are the control signals. Q_{max} is the maximum flow available for each control valve.
V_1 and V_2 are the actual sizes of the control volumes and are given by:

$$V_1 = A_{p_1} \cdot (l_{DE} - l_{1,min}) \tag{13}$$

$$V_2 = CR_2 \cdot A_{p_2} \cdot (h_2 - (l_{FG} - l_{2,min})) \tag{14}$$

where l_{DE} and l_{FG} are the actual lengths of the cylinders, derived from $\mathbf{r}_{DE}$ and $\mathbf{r}_{FG}$ given by (A.13) and (A.16) in appendix A.1. $l_{1,min}$ and $l_{2,min}$ are the collapsed lengths. CR_2 is the ratio between piston-side-area and the rod-side-area for cylinder 2 and h_2 is the cylinder stroke.

3.3 Wave Disturbance

The disturbance model describes the heave motion of the rig where the crane is located. The roll and pitch motions are not considered since the effect of these are less significant. The heave disturbance is described as a harmonic motion:

$$\ddot{y}_h(t) = -\omega_h^2 \cdot A_h \cdot \sin(\omega_h t) \tag{15}$$

where $\ddot{y}_h$ is the heave acceleration, A_h is the heave amplitude and ω_h is the heave frequency.
The heave acceleration acts on the system masses and yields a disturbance force for each mass, which can be described as generalised forces by means of (3). In this way the angular accelerations of the two crane jib, caused by the disturbance can be described as:

$$\begin{bmatrix} a_{11} & a_{12} \\ a_{21} & a_{22} \end{bmatrix} \cdot \begin{bmatrix} \delta\ddot{\phi}_1 \\ \delta\ddot{\phi}_2 \end{bmatrix} = \begin{bmatrix} \delta b_1 \\ \delta b_2 \end{bmatrix} \tag{16}$$

where $\delta\ddot{\phi}_1$ and $\delta\ddot{\phi}_2$ are the accelerations caused by generalised disturbance forces δb_1 and δb_2, which are given by (A.54)-(A.55) in appendix A.5. a_{11}, a_{12}, a_{21} and a_{22} are the same as in (4).

3.4 State-Space Representation

In order to establish a state-space model for the controller design, the mechanical and hydraulic models must be linearised.
The linearised equations of motion can be written as:

$$\ddot{\phi}_1 = \sum_{i=1}^{n} \frac{\partial}{\partial x_i} \left(\frac{b_1 \cdot a_{22} - a_{12} \cdot b_2}{D} \right) \Bigg|_{\mathbf{x}_{ss}} \cdot x_i^* \tag{17}$$

$$\ddot{\phi}_2 = \sum_{i=1}^{n} \frac{\partial}{\partial x_i} \left(\frac{a_{11} \cdot b_2 - b_1 \cdot a_{21}}{D} \right) \Bigg|_{\mathbf{x}_{ss}} \cdot x_i^* \tag{18}$$

where x_i is the i'th state variable, $\mathbf{x}_{ss}$ are the steady-state values of the state variables in the selected operating point. $x_i^* = x_i - x_{i,ss}$ which means that the linearised model relates to deviations of the state variables around the operating point.
The linearised flow continuity equations can be written as:

$$\dot{p}_1 = \frac{\beta_e}{V_1} \cdot Q_{max} \cdot u_1 - \sum_{i=1}^{n} \frac{\beta_e}{V_1} \cdot A_1 \cdot \frac{\partial v_1}{\partial x_i} \Bigg|_{\mathbf{x}_{ss}} \cdot x_i^* \tag{19}$$

$$\dot{p}_2 = \frac{\beta_e}{V_2} \cdot Q_{max} \cdot u_2 - \sum_{i=1}^{n} \frac{\beta_e}{V_2} \cdot A_2 \cdot \frac{\partial v_2}{\partial x_i} \Bigg|_{\mathbf{x}_{ss}} \cdot x_i^* \tag{20}$$

As seen from (13)-(14), V_1 and V_2 are also non-linear terms. Instead of linearising these, steady-state values will be calculated, which is assumed to be constant within a certain range around the selected operating point.
For the controller design the disturbance will represent a worst case situation by setting $A_h = 2m$ and $\omega_h = 0.5Hz$ giving a maximum heave acceleration of $\ddot{y}_h = 0.5m/s^2$. The angular accelerations caused by the disturbance can then be described similar to (5)-(6) in the following way:

$$\delta\ddot{\phi}_1 = \frac{\delta b_1 \cdot a_{22} - a_{12} \cdot \delta b_2}{D} \tag{21}$$

$$\delta\ddot{\phi}_2 = \frac{a_{11} \cdot \delta b_2 - \delta b_1 \cdot a_{21}}{D} \tag{22}$$

which are constant disturbances that can be scaled by an exogenous input.
The performance of the system is expressed by the exogenous output $\mathbf{z}$, which is the position, X_{tp} and Y_{tp}, of the crane's tool point and the control signals u_1 and u_2. The tool point position, denoted z_1 and z_2, is dependent on ϕ_1 and ϕ_2, a non-linear relation which needs to be linearised:

$$z_1 = \sum_{i=1}^{n} \left. \frac{\partial (X_{tp})}{\partial x_i} \right|_{\mathbf{x}_{ss}} \cdot x_i^* \tag{23}$$

$$z_2 = \sum_{i=1}^{n} \left. \frac{\partial (Y_{tp})}{\partial x_i} \right|_{\mathbf{x}_{ss}} \cdot x_i^* \tag{24}$$

The non-linear expressions for X_{tp} and Y_{tp} are given by (A.56) and (A.57) in appendix A.6.
The controller to be designed is a state-feedback type, and therefore the measured output $\mathbf{y}$ is simply all the states. Finally a state-space model can be established:

$$\begin{aligned}
\dot{\mathbf{x}} &= \mathbf{A} \cdot \mathbf{x} + \mathbf{B}_1 \cdot \mathbf{w} + \mathbf{B}_2 \cdot \mathbf{u} \\
\mathbf{z} &= \mathbf{C}_1 \cdot \mathbf{x} + \mathbf{D}_{11} \cdot \mathbf{w} + \mathbf{D}_{12} \cdot \mathbf{u} \\
\mathbf{y} &= \mathbf{C}_2 \cdot \mathbf{x} + \mathbf{D}_{21} \cdot \mathbf{w} + \mathbf{D}_{22} \cdot \mathbf{u}
\end{aligned}$$

where the state vector is $\mathbf{x} = [\phi_1 \ \dot{\phi}_1 \ \phi_2 \ \dot{\phi}_2 \ p_1 \ p_2]^T$, the exogenous input that controls the disturbance is $\mathbf{w}$ and the input vector is $\mathbf{u} = [u_1 \ u_2]^T$.
The system matrix has the following structure:

$$\mathbf{A} = \begin{bmatrix} 0 & 1 & 0 & 0 & 0 & 0 \\ A_{21} & A_{22} & A_{23} & A_{24} & A_{25} & A_{26} \\ 0 & 0 & 0 & 1 & 0 & 0 \\ A_{41} & A_{42} & A_{43} & A_{44} & A_{45} & A_{46} \\ A_{51} & A_{52} & 0 & 0 & 0 & 0 \\ A_{61} & A_{62} & A_{63} & A_{64} & 0 & 0 \end{bmatrix} \tag{25}$$

where the coefficients of the second row is obtained from (17), the coefficients of fourth row is obtained from (18), the coefficients of fifth row is the linearised terms of (19) and the coefficients sixth row consist is linearised terms of (20).
The input matrices have the following structure:

$$\mathbf{B}_1 = \begin{bmatrix} 0 \\ B_2 \\ 0 \\ B_4 \\ 0 \\ 0 \end{bmatrix}, \quad \mathbf{B}_2 = \begin{bmatrix} 0 & 0 \\ 0 & 0 \\ 0 & 0 \\ 0 & 0 \\ B_{51} & 0 \\ 0 & B_{62} \end{bmatrix} \tag{26}$$

where B_2 and B_4 are $\delta\ddot{\phi}_1$ and $\delta\ddot{\phi}_2$ from (21) and (22). B_{51} and B_{62} are the linear terms of (19) and (20).
The output matrices have the following structure:

$$\mathbf{C}_1 = \begin{bmatrix} C_{11} & 0 & C_{13} & 0 & 0 & 0 \\ C_{21} & 0 & C_{23} & 0 & 0 & 0 \\ 0 & 0 & 0 & 0 & 0 & 0 \\ 0 & 0 & 0 & 0 & 0 & 0 \end{bmatrix}, \quad \mathbf{C}_2 = \mathbf{I} \tag{27}$$

where the first row of $\mathbf{C}_1$ consist of the coefficients of (23) and the second row consist of the coefficients of (24).
The feedforward matrices are:

$$\mathbf{D}_{11} = 0, \quad \mathbf{D}_{12} = \begin{bmatrix} 0 & 0 \\ 0 & 0 \\ 1 & 0 \\ 0 & 1 \end{bmatrix}, \quad \mathbf{D}_{21} = 0, \quad \mathbf{D}_{22} = 0 \tag{28}$$

4. CONTROLLER DESIGN

Since the state-space model is a linearised description only valid within a certain range around the selected operating point, it is necessary to establish a series of state-space models and controllers for a series of selected operating point in order to cover the operation illustrated by Fig. 3. However, since the procedure for the controller design is the same for every operating point, only one controller will be designed here.
The selected operating point represents the first phase of the lifting operation - lifting the payload from the pipe deck. The initial position for the tool point is $(X_{tp}, Y_{tp}) = (25m, 0m)$ which, by inverse kinematics, gives the initial jib angles $\phi_1 = 0.1103rad$ and $\phi_2 = -1.4819rad$. Since the crane is only just about to move the initial angular velocities are $\dot{\phi}_1 = \dot{\phi}_2 = 0$. To maintain steady-state in the point, the hydraulic pressures must be calculated. Setting the rod-side pressures to $p_{r_1} = p_2 = 10bar$ the piston-side pressures are determined by static analysis to be $p_1 = 133bar$ and $p_{r_2} = 13bar$.
That is

$$\mathbf{x}_{ss} = [0.1103 \ 0 \ -1.4819 \ 0 \ 133 \ 10] \tag{29}$$

The undetermined coefficients in (25)-(27) for this operating point are given in Table 1.

Table 1. Model coefficients for selected operating point.

Coeff.		Value	Coeff.		Value
A_{21}	=	-0.7665	A_{52}	=	$-136.14 \cdot 10^3$
A_{22}	=	0	A_{61}	=	0
A_{23}	=	$9.831 \cdot 10^{-3}$	A_{62}	=	$-21.305 \cdot 10^3$
A_{24}	=	0	A_{63}	=	0
A_{25}	=	$3.958 \cdot 10^{-3}$	A_{64}	=	$21.305 \cdot 10^3$
A_{26}	=	$1.251 \cdot 10^{-3}$	B_2	=	0.025
A_{41}	=	$-9.165 \cdot 10^{-3}$	B_4	=	0.0037
A_{42}	=	0	B_{51}	=	$3.903 \cdot 10^3$
A_{43}	=	-0.6624	B_{62}	=	$1.869 \cdot 10^3$
A_{44}	=	0	C_{11}	=	-2.5868
A_{45}	=	$0.1302 \cdot 10^{-3}$	C_{13}	=	18.4269
A_{46}	=	$-4.221 \cdot 10^{-3}$	C_{21}	=	23.3572
A_{51}	=	0	C_{23}	=	1.6424

Given the plant:

$$\mathbf{P} \sim \left[\begin{array}{c|cc} \mathbf{A} & \mathbf{B}_1 & \mathbf{B}_2 \\ \hline \mathbf{C}_1 & \mathbf{D}_{11} & \mathbf{D}_{12} \\ \mathbf{C}_2 & \mathbf{D}_{21} & \mathbf{D}_{22} \end{array}\right] \tag{30}$$

a controller can be designed by following the procedure suggested by Abedor et al. (1995). Remembering the standards assumptions about $\mathbf{P}$ for state-feedback control:

(1) $\mathbf{C}_2 = \mathbf{I}$ and $\mathbf{D}_{21} = 0$.
(2) $\mathbf{A}$ and $\mathbf{B}_2$ are stabilisable.
(3) $\mathbf{C}_2$, $\mathbf{A}$ and $\mathbf{B}_1$ have no uncontrollable and unobservable modes on the imaginary axis.
(4) $\mathbf{D}_{12}^T \mathbf{C}_1 = 0$ and $\mathbf{D}_{12}^T \mathbf{D}_{12} = \mathbf{I}$

Then a controller $\mathbf{K}$ that solves the robust regulation problem with an H_∞ constraint for the plant $\mathbf{P}$ is given by:

$$\mathbf{K} \sim \left[\begin{array}{c|c} \tilde{\mathbf{A}} & \tilde{\mathbf{B}}[\mathbf{I} \ \mathbf{0}] \\ \hline \mathbf{B}_2^T \mathbf{L}^T \mathbf{W}^{-1} & -\mathbf{B}_2^T \mathbf{X} - \mathbf{B}_2^T \mathbf{L}^T \mathbf{W}^{-1} \mathbf{L} \end{array}\right] \tag{31}$$

$\tilde{\mathbf{A}}$ and $\tilde{\mathbf{B}}$ are the internal model matrices which depend on the type of input signal. For a step input:

$$\tilde{\mathbf{A}} = \mathbf{0}_{l \times l} \tag{32}$$

$$\tilde{\mathbf{B}} = \mathbf{I}_{l \times l} \tag{33}$$

where l is the number of signals of the output $\mathbf{y}$ to be controlled. Here $l = 2$, since the goal is to control the jib

angles ϕ_1 and ϕ_2 in order to track the tool point position given by $\mathbf{z}$. The control problem is illustrated by Fig. 5.

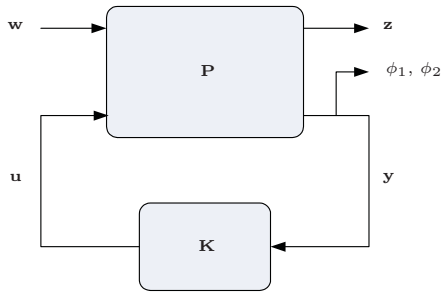

Fig. 5. P-K structure illustrating the control problem.

In (31) $\mathbf{L}$ is the unique solution to the Lyapunov equation:

$$\mathbf{L}\bar{\mathbf{A}} - \tilde{\mathbf{A}}\mathbf{L} = \tilde{\mathbf{B}} \tag{34}$$

where $\bar{\mathbf{A}} = \mathbf{A} + (\gamma^{-2}\mathbf{B}_1\mathbf{B}_1^T - \mathbf{B}_2\mathbf{B}_2^T)\mathbf{X}$. γ is a tuning parameter and $\mathbf{X}$ is the positive semidefinite stabilising solution to the Riccati equation:

$$\mathbf{A}^T\mathbf{X} + \mathbf{X}\mathbf{A} + \mathbf{X}(\gamma^{-2}\mathbf{B}_1\mathbf{B}_1^T - \mathbf{B}_2\mathbf{B}_2^T)\mathbf{X} + \mathbf{C}_1\mathbf{C}_1^T = 0 \tag{35}$$

In (31) $\mathbf{W}$ is the positive-definite solution satisfying the Lyapunov inequality:

$$\tilde{\mathbf{A}}\mathbf{W} + \mathbf{W}\tilde{\mathbf{A}}^T + \gamma^{-2}\mathbf{L}\mathbf{B}_1\mathbf{B}_1^T\mathbf{L}^T - \mathbf{L}\mathbf{B}_2\mathbf{B}_2^T\mathbf{L}^T < 0 \tag{36}$$

5. SIMULATION

The performance of the system with the implemented controller is simulated with MATLAB/Simulink®. The simulation shows the performance of the controller in the situation where the tool point is to move up $0.5m$ in a straight line. The state-space model is assumed to be representative during the whole operation.
The reference signals are calculated by inverse kinematics for the new point $(X_{tp}, Y_{tp}) = (25m, 0.5m)$ which gives the new jib angles $\phi_1 = 0.1315rad$ and $\phi_2 = -1.4786rad$. Since the state-space model relates to deviations of the state variables, the reference signals are determined by subtracting the angles for initial point from the angles for the new point:

$$\phi_{1_{ref}} = \phi_{1_{new}} - \phi_{1_{ini}} = 0.0212rad \tag{37}$$

$$\phi_{2_{ref}} = \phi_{2_{new}} - \phi_{2_{ini}} = 0.0033rad \tag{38}$$

Setting the tuning parameter $\gamma = 1$ the controller is found to be:

$$\mathbf{K} \sim \left[\begin{array}{c|c} \mathbf{A}_K & \mathbf{B}_K \\ \hline \mathbf{C}_K & \mathbf{D}_K \end{array}\right] \tag{39}$$

where

$$\mathbf{A}_K = \begin{bmatrix} 0 & 0 \\ 0 & 0 \end{bmatrix}, \quad \mathbf{B}_K = \begin{bmatrix} 1 & 0 & 0 & 0 & 0 & 0 \\ 0 & 1 & 0 & 0 & 0 & 0 \end{bmatrix}, \quad \mathbf{C}_K = \begin{bmatrix} -0.0021 & 0 \\ -0.0005 & 0 \end{bmatrix} \tag{40}$$

$$\mathbf{D}_K = \begin{bmatrix} -22.757 & -0.094 & -3.949 & -0.221 & -0.0004 & 0.0004 \\ -5.643 & 0.108 & 17.797 & 0.639 & 0.0002 & -0.0016 \end{bmatrix} \tag{41}$$

In the simulation the reference is given as a step input, which the system should track as fast and precise as possible without introducing instability.
Tracking of the relative tool point position is illustrated in Fig. 6 both with and without the heave disturbance.

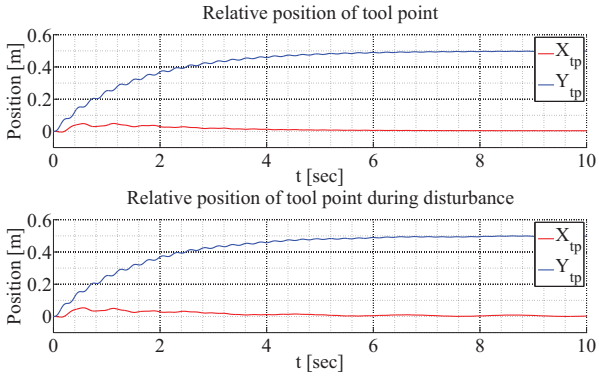

Fig. 6. Tracking of tool point.

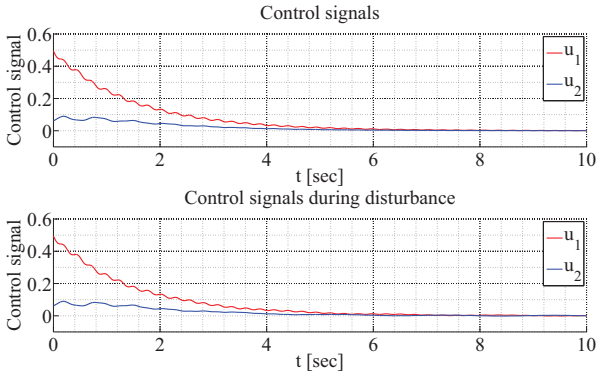

Fig. 7. Control signals.

The designed controller yields good tracking and disturbance attenuation, however the response is slow.
The usage of H_∞ control signal is illustrated in Fig. 7. This reveals the reason for slow response, since only half of the available flow is utilised. The controller guaranties stability, however in this case the controller design might be too conservative, sacrificing the system performance.
To attenuate the disturbance the control signal becomes negative in certain periods. For this model this is not physical meaningful, since the flow control valves in Fig. 4 is unidirectional. To deal with this phenomena, a saturation of the control signal must be introduced or the hydraulic model must be extended to include more of the physical system's capabilities.

6. CONCLUSIONS

The purpose of the presented work has been to investigate if an advanced control method can be applied to achieve satisfactory performing tool point control for a hydraulically actuated knuckle boom crane. The designed controller shows good tracking performance and robustness, but is rather slow reacting. Compared to other and more conventional methods for tool point control, this is not satisfactory. However by including additional techniques, such as loop shaping, in the design approach, the performance is likely to be improved. This is one relevant task for future work.
Other targets for future work is to extend the hydraulic model to include more of the functionalities of the physical system, and thereby improving the capabilities of the con-

troller. Finally it must be possible to handle more complete duty cycles than the one the controller has been designed for. As mentioned in section 4, this may be solved by making a gain schedule from several models and controllers for a number of operating points representing the operation to be considered. Another approach is to reformulate the crane model as a *linear parameter varying* (LPV) model and apply the presented design approach to this model. If the controller performance can be improved, the LPV approach is indeed worth investigating, since it offers a smooth variation of controller gain during operation of the crane.
Alternatively, other control strategies, such as feedback linearisation or sliding-mode control, may be considered. Both strategies have succesfully been applied in other crane control problems by Park et al. (2007) and Ngo and Hong (2011), respectively.

REFERENCES

Abedor, J., Nagpal, K., Khargonekar, P.P., and Poolla, K. (1995). Robust regulation in the presence of norm-bounded uncertainty. *IEEE Transactions on Automatic Control*, 40(1), 147–153.

Burul, I., Kolonic, F., and Matusko, J. (2010). The control system design of a gantry crane based on h-infinity control theory. *MIPRO, 2010 Proceedings of the 33rd International Convention, Opatija, Croatia*, 183–188.

Ebbesen, M.K., Hansen, M.R., and Andersen, T.O. (2006). Optimal tool point control of hydraulically actuated flexible multibody system with an operator-in-the-loop. *III European Conference on Computational Mechanics, Solids, Structures and Coupled Problems in Engineering, Lisbon, Portugal*, 568–568.

Iwasa, T., Terashima, K., Jian, N.Y., and Noda, Y. (2010). Operator assistance system of rotary crane by gain-scheduled h-infinity controller with reference governor. *2010 IEEE International Conference on Control Applications, part of 2010 IEEE Multi-Conference on Systems and Control, Yokohama, Japan*, 1325–1330.

Krus, P. and Palmberg, J.O. (1992). Vector control of a hydraulic crane. *Procedings of the International Off-Highway and Powerplant Congress and Exposition, Millwaukee, USA*.

Mattila, J. and Virvalo, T. (2000). Energy-efficient motion control of a hydraulic manipulator. *Procedings of the 2000 IEEE International Conference on Robotics and Automation, San Fransisco, USA*, 3000–3006.

Moradi, H., Hajikolaei, K.H., and Bakhtiari-Nejad, F. (2009). Robust h-infinity control of an over-head crane system with parametric uncertainties. *Proceedings of the ASME International Design Engineering Technical Conferences and Computers and Information in Engineering Conference, San Diego, USA*, 377–384.

Munzer, M.E. (2003). Resolved motion control of mobile hydraulic cranes. *Ph.D. Thesis, Aalborg University.*

Ngo, Q. and Hong, K.S. (2011). Sliding-mode antisway control of an offshore container crane. *IEEE/ASME Transaction on Mechatronics*, 16.

Park, H., Chwa, D., and Hong, K.S. (2007). A feedback linearization control of container cranes: varying rope length. *International Journal of Control, Automation and Systems*, 5(4), 379–387.

Pedersen, M.M., Hansen, M.R., and Ballebye, M. (2010). Developing a tool point control scheme for a hydraulic crane using interactive real-time dynamic simulation. *Modeling, Identification and Control*, 31(4), 133–143.

Appendix A. MODEL DESCRIPTION

The appendix presents comprehensive expressions of the equations derived to establish the model of the crane's mechanical systems. It also contains expressions for the disturbance model and tool point kinematics. To view the appendix please go to:

`http://www.uia.no/en/portals/`
`about_the_university/engineering_and_science/`
`-_engineering/-_-_mechatronics/bak`

and select the link for pulication [C3] on the list.